

# Is the central binary system of the planetary nebula Henize 2–428 a Type Ia supernova progenitor?

Enrique García-Berro<sup>a,b</sup>, Noam Soker<sup>c</sup>, Leandro G. Althaus<sup>d</sup>, Ignasi Ribas<sup>e,b</sup>, Juan C. Morales<sup>e,b</sup>

<sup>a</sup>*Departament de Física Aplicada, Universitat Politècnica de Catalunya, c/Esteve Terrades 5, 08860 Castelldefels, Spain*

<sup>b</sup>*Institut d'Estudis Espacials de Catalunya, c/Gran Capità 2–4, Edif. Nexus 104, 08034 Barcelona, Spain*

<sup>c</sup>*Department of Physics, Technion – Israel Institute of Technology, Haifa 32000, Israel*

<sup>d</sup>*Facultad de Ciencias Astronómicas y Geofísicas, Universidad Nacional de La Plata–IALP-CONICET, Paseo del Bosque s/n, 1900 La Plata, Argentina*

<sup>e</sup>*Institut de Ciències de l'Espai–CSIC, Campus UAB, Facultat de Ciències, Torre C5 – parell – 2a planta 08193 Bellaterra, Spain*

---

## Abstract

We critically discuss the recent observations of the binary system at the center of the bipolar planetary nebula Henize 2–428. We find that the proposed explanation of two equal-mass degenerate objects with a total mass larger than the Chandrasekhar limiting mass that supposedly will merge in less than a Hubble time, possibly leading to a SN Ia, is controversial. This hypothesis relies on the assumption that the variability of the He II 5412 Å spectral line is due to two absorption components. Instead, we propose that it can be accounted for by a broad absorption line from the central system on top of which there is a narrow emission line from the nebula. This prompted us to study if the binary system can be made of a degenerate star and a low-mass main sequence companion, or of two degenerate objects of smaller mass. We find that although both scenarios can account for the existence of two symmetric broad minima in the light curve, the second one agrees better

---

*Email addresses:* [enrique.garcia-berro@upc.edu](mailto:enrique.garcia-berro@upc.edu) (Enrique García-Berro), [soker@physics.technion.ac.il](mailto:soker@physics.technion.ac.il) (Noam Soker), [althaus@fcaglp.fcaglp.unlp.edu.ar](mailto:althaus@fcaglp.fcaglp.unlp.edu.ar) (Leandro G. Althaus), [iribas@ice.csic.es](mailto:iribas@ice.csic.es) (Ignasi Ribas), [morales@ieec.uab.es](mailto:morales@ieec.uab.es) (Juan C. Morales)

with observations. We thus argue that the claim that Henize 2–428 provides observational evidence supporting the double-degenerate scenario for SN Ia is premature.

*Keywords:* Planetary nebulae, Stars: AGB and post-AGB, Supernovae, White dwarfs

---

## 1. Introduction

Thermonuclear, or Type Ia supernovae (SNe Ia), are the result of the explosion of carbon-oxygen white dwarfs. Despite their well known observed properties, the nature of the progenitor systems that produce a SNe Ia event has not been hitherto elucidated, and several scenarios have been proposed, none of which gives a satisfactory answer to all the abundant observational material. The scenarios can be classified into six categories — see, for instance, Tsebrenko & Soker (2015) for a recent discussion of some of the channels, and Wang & Han (2012) and Maoz et al. (2014) for extended reviews of some of these scenarios.

As there is no consensus on which are the SN Ia progenitor(s), it is crucial to refer to all scenarios (or categories of scenarios) when confronting them with observations. We list them in alphabetical order, and cite only a few references for each scenario: a) The core-degenerate (CD) scenario (Livio & Riess, 2003; Kashi & Soker, 2011; Soker et al., 2013), b) The double-degenerate (DD) scenario (e.g., Webbink 1984; Iben & Tutukov 1984), c) The double-detonation (DDet) mechanism (e.g., Woosley & Weaver 1994; Livne & Arnett 1995; Shen et al. 2013. d) The single-degenerate (SD) scenario (e.g., Whelan & Iben 1973; Nomoto 1982; Han & Podsiadlowski 2004), e) The recently proposed singly-evolved star (SES) scenario (Chiosi et al., 2015), and f) The WD-WD collision (WWC) scenario (e.g., Raskin et al. 2009; Thompson 2011; Kushnir et al. 2013; Aznar-Siguán et al. 2013).

Since all these scenarios involve white dwarfs, all progenitors evolve through one or two planetary nebula (PN) phases. Accordingly, one of the pieces of evidence that would help in constraining SN Ia scenarios is to study PNe. Furthermore, in some cases SN Ia have been even claimed to take place inside planetary nebulae (e.g., Dickel & Jones 1985; Tsebrenko & Soker 2013, 2015), a process termed SNIP.

In a recent paper Santander-García et al. (2015) analyzed the central binary system of the planetary nebula Henize 2–428 (Rodríguez et al., 2001;

Santander-García et al., 2011). Santander-García et al. (2015) found that the light curve of this PN shows two nearly identical broad minima, indicating significant tidal distortion of the components of binary system, and that there is an absorption line of He II 5412 Å that varies with time. Given that the two minima of the light curve are practically identical, they assumed that they are caused by a binary system composed of two equal-mass stars of the same type, and found the temperature, radius, and luminosity, of the two stars to be almost identical. They further argued that most likely these are two degenerate stars, i.e., white dwarfs or cores of post-asymptotic giant branch (AGB) stars, on their way to become CO white dwarfs. As the combined mass in this model is  $1.76 M_{\odot}$ , Santander-García et al. (2015) further argued that these two stars will merge to form a SN Ia in the frame of the DD scenario.

Here we critically discuss the explanation of Santander-García et al. (2015). As we explain in Sect. 2 we find the interpretation of the observations of Santander-García et al. (2015) to be plausible, albeit other possibilities are conceivable. In Sect. 3 we relax the assumptions of these authors and we propose alternative models of the binary system. The first of these models consists of binary system in which only one of the components is a degenerate star, while the secondary star is normal non-evolved star. The second of the models involves two non-identical degenerate stars, but with a combined mass smaller than the Chandrasekhar limiting mass. A short summary is given in Sect. 4.

## 2. Preliminary considerations

### 2.1. A binary system made of two identical stars?

Santander-García et al. (2015) argue for a binary system composed of two stars having the same mass,  $0.88 \pm 0.13 M_{\odot}$ , the same luminosity,  $\approx 420 L_{\odot}$  at a distance of 1.4 kpc, and the same radius,  $0.68 \pm 0.04 R_{\odot}$ . This implies that the two stars are at the same evolutionary stage. However, any small difference in the main sequence mass will turn to a large one on the asymptotic giant branch (AGB). An AGB star having a core of  $0.88 M_{\odot}$  burns hydrogen at a rate of  $\sim 2 \times 10^{-7} M_{\odot} \text{ yr}^{-1}$  (e.g., Paczyński 1970). For a difference in mass between the two cores  $< 0.02 M_{\odot}$  the difference of evolutionary times between the post-AGB stars should be  $\lesssim 10^5 \text{ yr}$ . This requires a mass difference on the main sequence of  $\Delta M/M \lesssim 10^{-3}$ , depending on the initial mass of the stars.

It could be argued that there are other binary systems with almost identical components, known as twin binaries (Lucy & Ricco, 1979). Specifically, Pinsonneault & Stanek (2006) studied 21 detached eclipsing binaries in the Small Magellanic Cloud and found that 50% of detached binaries have companions with very similar masses. However, Lucy (2006) and Cantrell & Dougan (2014) concluded that there is a strong observational bias that affects spectroscopically selected binary stars, and that the apparent overabundance of twin binaries does not reflect their true population. In summary, the case for a twin binary is possible, but unlikely, hence motivates us for a careful reexamination of such a claim.

## 2.2. Stellar properties

As mentioned, in the model proposed by Santander-García et al. (2015) each star is a post-AGB star with a mass of  $0.88 M_{\odot}$ . When a post-AGB of that mass fades to a luminosity of  $\approx 10^3 L_{\odot}$  its radius is already  $\simeq 0.02 R_{\odot}$  (e.g., Bloeker & Schoenberner 1991). This radius is about 30 times smaller than the radius suggested by Santander-García et al. (2015). This poses a serious problem to their model.

In the first of our models we investigate a case where the luminosity of the system is due to just one star, and the luminosity of the companion is negligible — see below for more details. At a distance of  $D = 1.4$  kpc as deduced by Santander-García et al. (2015) the luminosity is  $\approx 850 L_{\odot}$ . This can be a star whose evolution was truncated on the upper red giant branch (RGB), when its core mass was only  $M_1 \approx 0.45 M_{\odot}$ , or on the lower AGB when its core mass was  $\approx 0.5 M_{\odot}$ . On the other hand, if the distance is larger, say  $D = 1.8$  kpc, the luminosity is  $\approx 1.4 \times 10^3 L_{\odot}$ . This can be a star whose evolution was truncated on the lower AGB, when its core mass was only  $M_1 \approx 0.52 - 0.55 M_{\odot}$ . In our proposed model the companion that terminated the RGB or the AGB evolution of the primary component is a main sequence star of  $\sim 0.3 - 0.5 M_{\odot}$ . In the second of our models we assume that indeed both stars are post-AGB stars but we allow the stars to have different physical parameters, namely different masses, effective temperatures and luminosities.

A note is in place here on the distance to Henize 2-428. Santander-García et al. (2015) provided a rough estimate of the distance of  $1.4 \pm 0.4$  kpc based on the dereddened apparent magnitudes of Henize 2-428. Maciel (1984) obtained a distance of 1.7 kpc, Cahn & Kaler (1971) derived a distance of 2.7 kpc,

while the most recent determination of Frew et al. (2015), using the H $\alpha$  surface brightness–radius relation is also 2.7 kpc. Based on these values we will scale our expressions with two distances,  $D = 1.4$  kpc and  $D = 1.8$  kpc, as the value adopted by Santander-García et al. (2015) was obtained from their fit to the properties of the binary system, which is questioned here.

### 2.3. Light curves and spectrum

The arguments of Santander-García et al. (2015) for their claim of a binary system of equal-mass stars at the same evolutionary stage are the nearly identical minima in the light curve, and the line profile of the He II 5412 Å spectral feature — see their figures 2 and 3. The nearly identical minima of the light curve have been suggested to be indicative that both members of the binary system have very similar masses. Additionally, Santander-García et al. (2015) found that the He II 5412 Å spectral line of Henize 2–428 is variable. They attributed the variability of this line to Doppler shifts of two equal-mass stars, and then used two Gaussian absorption profiles to model the variation. Consequently, in their joint analysis of the light curve and the spectrum they *forced* the mass ratio  $q = M_2/M_1$  of the binary system to be 1. Furthermore, Santander-García et al. (2015) *did not model the spectra* of both components of the binary system, since they were not able to measure surface gravities for each one of the individual binary members. Finally, they *assumed* that both stars are at the same evolutionary stage. All of these assumptions are critical in their analysis.

In particular, it must be stressed that even if the mass ratio is close to 1, the nature of the stars can be very different, and that the lack of determinations of surface gravities leaves room for alternative explanations. In particular, a close look at figures 2 and 3 of Santander-García et al. (2015) suggests that the spectrum of Henize 2–428 can be explained by assuming that there is an emission line on top of the absorption profile. We therefore examine a possible alternative interpretation where the line profile is the result of a wide absorption line belonging to the primary star, and a narrow emission line coming from the compact dense nebula reported by Rodríguez et al. (2001), or which originates even much closer to the star from the wind itself. In this alternative explanation both emission and absorption lines change with orbital phase. This is not unusual. Many central stars of planetary nebulae show He II absorption lines (e.g., Weidmann & Gamen 2011). The emission line is seen in some nebulae, e.g., in Abell 48 whose central star is a WN star (Todt et al., 2013). Most interestingly, in the study of Weidmann & Gamen

(2011) there are several PNe that show a wide He II 5412 Å absorption line with a weak emission feature in the center of the wide absorption line. This forms a spectral structure similar to that of Henize 2–428. The most noticeable examples of this are the PNe He 2–105, He 2–434, and to some degree SP 3 and PC 12. All these central stars are O stars. To these we add the PN Pa 5, for which the central star shows a wide He II 5412 Å absorption line and the resolved nebula shows a narrow He II 5412 Å emission line (García-Díaz et al., 2014). Another relevant case is the central star of the Eskimo planetary nebula (NGC 2392). The He II 5412 Å line shows a structure similar to that of Henize 2–428 (Prinja & Urbaneja, 2014). This structure varies on time scales down to about an hour. Prinja & Urbaneja (2014) attribute the variation in the line to a variable distribution of clumps in the wind, variations in the velocity field, and/or the mass loss rate, rather than to a binary star.

It could be argued that if our interpretation is correct, and the He II 5412 Å emission line is nebular, a He II 4686 Å emission line should be also observed, but it is not. However, other PNe, like He 2–105, PC 12, He 2–434 and SP 3 have spectra with weak He II 5412 Å bumps (which we interpret as an emission line) in the center of a broad absorption line, whereas the He II 4686 Å line is in absorption (Weidmann & Gamen, 2011). On the other hand, in the PN M 1–14 the He II 5412 Å line is in absorption but the He II 4686 Å occurs in emission (Weidmann & Gamen, 2011). These cases show that there is an interplay between emission and absorption in the He II lines. This suggests that the emission region, like the absorption one, is located very close to the star, but not at the same place. In all these cases both the absorption and emission features vary with orbital phase. In conclusion, based on the current observations the existence of a He II emission line on top of the broad absorption feature cannot be discarded, and needs to be considered.

Furthermore, Santander-García et al. (2015) established an upper limit on the effective temperature of the members of the binary system of  $\approx 40,000$  K, based on the absence of a He II 5412 Å emission line, but there are many PNe whose central stars have effective temperatures larger than 40,000 K and do not have He II emission lines. Since we assume that the emission line is indeed present in the spectrum, the upper limit of Santander-García et al. (2015) to the effective temperature is no longer valid, and the effective temperature could be sufficiently large to allow emission. Consequently, in the following we will scale quantities with an effective temperature  $T_{\text{eff}} = 45,000$  K.

### 3. Possible binary models

According to all the considerations put forward in the previous section, here we explore two models in which the mass ratio is  $\approx 1$ , but with different characteristics. The first of these models involves a semi-detached system in which the members of the binary system are not at the same evolutionary stage, while for the second model we adopt an overcontact binary system made of two post-AGB stars, as Santander-García et al. (2015) did, but with less restrictive assumptions.

#### 3.1. A semi-detached binary system

We first examine a binary model where the secondary is a main sequence star of mass  $M_2 \simeq 0.3 - 0.5 M_\odot$ . If we take the primary to be a post-RGB star of mass  $M_1 \simeq 0.45 M_\odot$  or a post-AGB of mass  $M_1 \simeq 0.55 M_\odot$  (e.g., Bloeker 1993), then these two cases span a mass ratio of  $q = M_2/M_1 \simeq 0.6 - 1.0$ . Using the expression for the Roche lobe radius  $r_L$  from Eggleton (1983), we find for the primary star  $r_{L1}/a = 0.42$  and  $0.38$  for  $q = M_2/M_1 = 0.6$  and  $1.0$ , respectively, where  $a$  is the orbital separation. For the secondary star we find  $r_{L2}/a = 0.34$  and  $0.38$  for  $q = M_2/M_1 = 0.6$  and  $1$ , respectively. For an orbital period of  $P = 4.2$  h the orbital separation (for a circular orbit) is  $a = 1.27(M/0.9 M_\odot)^{1/3} R_\odot$ , and the Roche lobe of the primary star is

$$r_{L1} = 0.51 \left( \frac{M}{0.9 M_\odot} \right)^{1/3} \left( \frac{r_L/a}{0.4} \right) R_\odot, \quad (1)$$

where  $M = M_1 + M_2$  is the total binary mass. From the primary luminosity,  $L_1 = 845(D/1.4 \text{ kpc})^2 L_\odot$ , and for the effective temperature assumed here, the primary radius is

$$R_1 = 0.48 \left( \frac{D}{1.4 \text{ kpc}} \right) \left( \frac{T_1}{4.5 \times 10^4 \text{ K}} \right)^{-2} R_\odot. \quad (2)$$

For a distance of  $D = 1.8$  kpc the primary radius with that effective temperature is  $R_1 = 0.62 R_\odot$ , but taking a temperature  $T_1 = 50,000$  K will make the primary just filling in its Roche lobe. In our model the primary is close to filling its Roche lobe (assuming synchronization). For the secondary the Roche lobe radius is in the range  $r_{L2} \simeq 0.42 - 0.5 R_\odot$ . Thus, the secondary also touches its Roche lobe.

We consider two possible evolutionary scenarios. We prefer the post-RGB one, but cannot rule out the post-AGB one. We first describe the relevant



evolutionary tracks on the Hertzsprung-Russell diagram, and then turn to discuss the two possible scenarios. The last step of our analysis consists of computing the light curve of the proposed binary system.

### 3.1.1. Evolutionary tracks

In the top panel of Fig. 1 we present some relevant evolutionary tracks on the Hertzsprung-Russell diagram, together with the approximate location of the central star of Henize 2–428 at two distances,  $D = 1.4$  kpc (square) and  $1.8$  kpc (asterisk), and the position reported by Santander-García et al. (2015), circle. The sequences of masses  $M_1 = 0.57$  and  $0.87 M_\odot$  were taken from Renedo et al. (2010), and are the result of the full evolution of zero-age main sequence (ZAMS) stars with masses  $M_{\text{ZAMS}_1} = 1.5$  and  $5.0 M_\odot$ , respectively, of Solar metallicity. The evolution is followed through all the relevant stages, including the hydrogen and helium core burning phases, the thermally-pulsing AGB phase, and the post-AGB evolution to the white dwarf stage. The  $M_1 = 0.504 M_\odot$  sequence was also taken from Renedo et al. (2010), and corresponds to a progenitor of mass  $M_{\text{ZAMS}_1} = 0.85 M_\odot$  with  $Z = 0.001$ . In addition, the post-RGB evolution of a  $0.432 M_\odot$  helium-core low-mass white dwarf is included. This sequence is the result of the non-conservative binary evolution of a star of mass  $M_{\text{ZAMS}_1} = 1.0 M_\odot$  that abandons the RGB before the onset of core helium burning (Althaus et al., 2013). Finally, the evolutionary track of a  $M_1 = 0.84 M_\odot$  post-AGB remnant of a  $M_{\text{ZAMS}_1} = 3.0 M_\odot$  progenitor with metallicity  $Z = 0.001$  that experiences a late thermal pulse (LTP) when its effective temperature was  $T_{\text{eff}} = 10,000$  K is shown as well. As a result of the LTP, the post-AGB remnant experiences a fast evolution to the blue. After reaching a maximum effective temperature, this remnant evolves back to the domain of giant stars.

Note that the luminosity inferred for Henize 2–428, for the effective temperatures used by Santander-García et al. (2015) and by us, is substantially smaller than that predicted by post-AGB evolutionary models for masses of  $M_{\text{ZAMS}_1} \gtrsim 0.55 M_\odot$ . The claimed masses for the two central stars of Henize 2–428 do not fit the other claimed properties of the stars in the model proposed by Santander-García et al. (2015). However, the  $M_1 = 0.504 M_\odot$  post-AGB star presented here (upper panel) experiences an LTP at  $T_{\text{eff}} = 48,000$  K, which brings the remnant back rapidly to the red giant domain and finally to the white dwarf stage. Such an evolutionary track covers the general region of Henize 2–428 on the Hertzsprung-Russell diagram.

Finally, the bottom panel of Fig. 1 displays the evolution of a star with



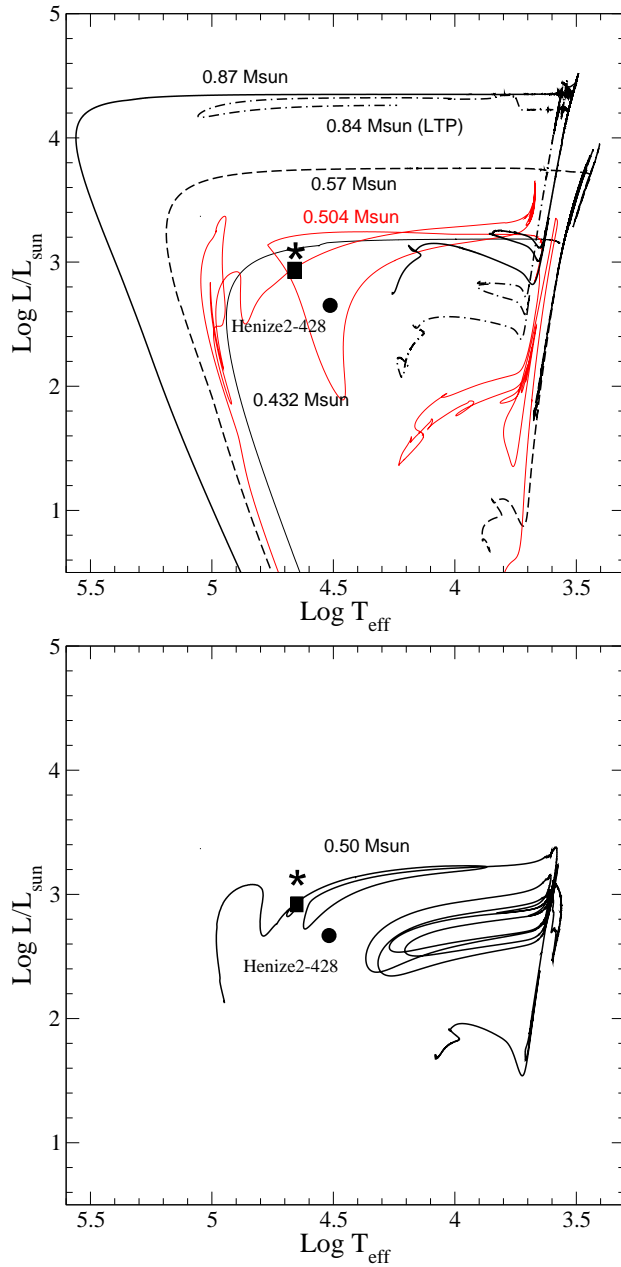


Figure 1: Relevant evolutionary tracks (see text for details). Marked are the location of each of the two identical stars of Henize 2–428 according to the model of Santander-García et al. (2015), filled circle, and the central star in our proposed scenario when the distance is  $D = 1.4$  kpc (filled square) and when  $D = 1.8$  kpc (asterisk).

$M_{\text{ZAMS}_1} = 2.5 M_{\odot}$ , and  $Z = 0.01$ . The evolution of this star was truncated on the lower AGB, when its luminosity is  $L = 1.4 \times 10^3 L_{\odot}$ , the observed luminosity of the binary system for the distance we adopt. At this point mass was removed to mimic a common-envelope episode. The final mass of the remnant after this intense episode of mass loss is  $0.50 M_{\odot}$ . The evolution in the Hertzsprung-Russell diagram of this sequence shows several blue loops, which are due to successive ignitions of the hydrogen shell. As can be seen, this track is also able to reproduce the observed position of Henize 2–428, for our adopted distance.

In conclusion, post-RGB helium-core remnants with stellar masses of  $M_1 \approx 0.45 M_{\odot}$  and low-mass cores of AGB stars that truncate the lower AGB with masses of  $M_1 \approx 0.50 - 0.55 M_{\odot}$  can account for the central star of Henize 2–428.

### 3.1.2. *Post-RGB evolution*

Guerrero et al. (2000) studied 15 bipolar PNe, and only in Henize 2–428 they detect no  $\text{H}_2$  emission, and it was the only PN in their sample in which a bright central star was found. It seems there is something strange in the evolution of this PN, which here is attributed to the system being a post-RGB star. Rodríguez et al. (2001) found the low abundances of most elements they study (relative to hydrogen) of Henize 2–428 to be similar to those found for PNe belonging to the Galactic halo. They suggested that this points to a low-mass progenitor. It is quite possible that the central star of Henize 2–428 is a post-RGB star orbited by a low-mass main sequence star. The post-RGB scenario is compatible with the low nebular mass, as the initial stellar mass in this scenario is  $M_{\text{ZAMS}_1} \approx 1 M_{\odot}$ , and the post-RGB mass is  $M_1 \approx 0.45 M_{\odot}$ .

### 3.1.3. *Post-AGB evolution*

In this proposed alternative scenario the evolution of the primary star is truncated on the lower AGB when its luminosity is between  $\approx 10^3$  and  $1.5 \times 10^3 L_{\odot}$  and its radius is  $\approx 150 R_{\odot}$ , assuming in this case a distance of  $D = 1.8$  kpc. The core mass is  $\approx 0.50 - 0.55 M_{\odot}$  (e.g., Bloeker 1993; Fig. 1 here). The companion will spiral-in due to tidal forces when the primary radius is about quarter of the orbital separation (Soker, 1996). The initial orbital separation in this scenario is therefore  $a_0 \approx 3$  AU.

To avoid engulfment already on the RGB phase of the primary star, the primary size on the RGB must be  $< 10^2 R_{\odot}$ , which limits the initial mass

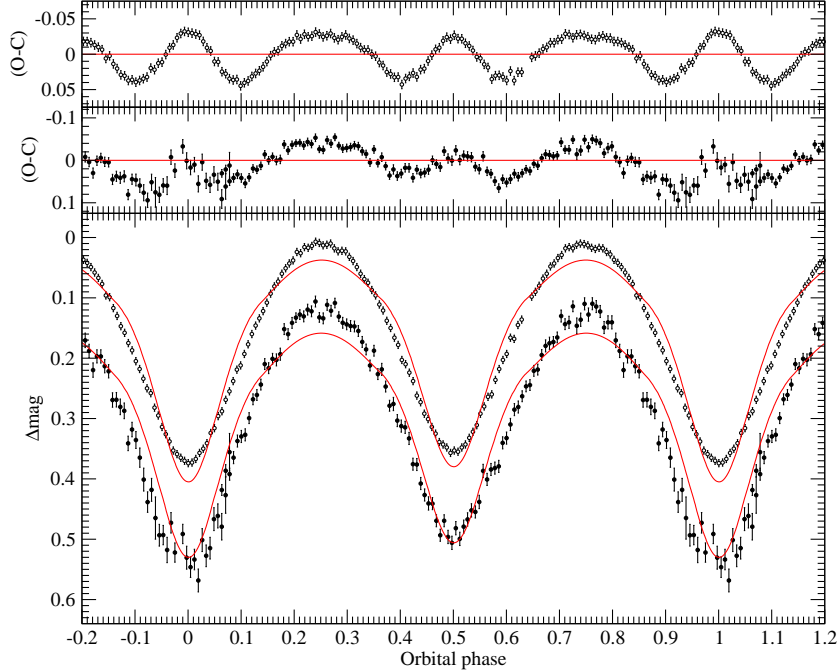


Figure 2: Light curve fit assuming a semidetached binary system made of a degenerate core and a main sequence companion, with the primary component filling the Roche lobe. B- and I-band light curves are shown in the lower panel using filled and open circles, respectively. Red lines are the best-fit models for each band. Residuals are shown in the upper panels. Note the different scale for each band.

of the primary star to be  $2.3 \lesssim M_{\text{ZAMS}_1}/M_{\odot} \lesssim 6.0$  (Iben & Tutukov, 1985). Therefore, in this scenario the AGB star is more massive, and a more massive nebula is expected.

#### 3.1.4. Light curve

Now the natural question is whether this model is consistent with the observations of Santander-García et al. (2015). Clearly, in our model both components of the binary system have similar masses, and the stars are very close. Thus, the minima of the light curve will be broad, as a consequence of tidal distortion of the components of the binary system. This is in accordance with the observed light curve obtained by Santander-García et al. (2015). However, there is a fundamental difference between our model and that of Santander-García et al. (2015). Due to the large luminosity contrast between

	Primary	Secondary
$M (M_{\odot})$	0.495	0.396
$R (R_{\odot})$	0.506	0.438
$r$ pole	0.3748	0.3226
$r$ point	0.5230	0.4044
$r$ side	0.3949	0.3406
$r$ back	0.4250	0.3669

Table 1: Absolute masses and volumetric radii derived from the best fit to light curves assuming a semi-detached binary system. For each component, the radius relative to the semimajor axis is given in different directions accounting for deformation: towards the pole ( $r_{\text{pole}}$ ) and towards the companion direction ( $r_{\text{point}}$ ), opposite ( $r_{\text{back}}$ ), and perpendicular to the orbital plane ( $r_{\text{side}}$ ).

the evolved object and the main sequence star, in our model the secondary star can be easily unnoticed in a first analysis, and the minima of the light curve are due to ellipsoidal variations of the post-AGB star. However, the light curve of this binary system can be easily confused with that of a binary system in which both components are post-AGB stars.

To check whether our model is consistent with the observed data we computed synthetic light curves for this model. We used the latest version of the Wilson-Devinney code (Wilson & Devinney, 1971; Wilson, 1979). This code allows to fit several light curves simultaneously providing parameters that are consistent with all the observed data. We have used the B- and I-band light curves of Henize 2–428 to get the orbital and physical parameters of the system. Specifically, we obtained the inclination with respect the visual plane ( $i$ ), the pseudo-potentials ( $\Omega_1$  and  $\Omega_2$ ), from which the radii of the components can be computed, the temperature of the secondary component ( $T_{\text{eff},2}$ ), the luminosity ratio for each bandpass ( $L_2/L_1$ ), and a phase shift to account for period inaccuracies. Square-root limb-darkening coefficients were interpolated in the tables of Claret (2000a), and adjusted dynamically according to the current temperatures and surface gravities of the stars at each iteration. The reflection albedos were fixed at 1.0, appropriate for stars with radiative envelopes, and the gravity darkening exponents were set to 1.0, following Claret (200b). The best fit is obtained by differential corrections, iterating until the internal errors of the parameters are smaller than the corrections applied in three consecutive iterations and repeating this process

five times, selecting as best fit that with the smaller residuals.

For this model we fixed the orbital separation to  $a = 1.27 R_{\odot}$ , which corresponds to the observed period  $P = 0.1758$  days. For the effective temperature of the primary we adopted  $T_{\text{eff},1} = 45,000$  K, as explained in Sect. 3.1. Finally, the mass ratio was kept fixed at  $q = 0.8$ . We fixed the primary component pseudo-potential to its critical value ( $\Omega_1=3.42$  according to the mass ratio) to force a semi-detached configuration and we tested fits with fixed values of  $\Omega_2$  in steps of 0.1. This was done in order to prevent convergence towards an overcontact system if  $\Omega_2$  is set free. Nevertheless, the best fit was found close to the limit of overcontact with  $\Omega_2 = 3.50$ . Figure 2 and Table 1 show, respectively, the light curves in the B- and I-band, and the relevant physical parameters of the best-fit solution. The best fit model has an inclination  $i = 69.792^\circ$ , a phase shift of 0.0008, and the effective temperature of the secondary star is  $T_{\text{eff},2} = 41,220$  K. Finally, the ratio of the luminosity of the secondary star and the primary component is 0.683 in the B-band, and 0.679 in the I-band. Although the residuals of the fit are rather small (32.65 mmag in the B-band, and 23.51 mmag in the I-band), the top panel of Fig. 2 shows that there are systematic departures of the computed light curve from the observed one, which can be also easily noticed near the maxima and minima of the light curve in the bottom panel of this figure. We also tested different mass ratios, from 0.6 to 1.0, but the light curve fits were not significantly better.

Clearly, the best-fit model is at odds with our initial hypothesis. Most significantly, the best-fit model shows that the luminosity of the secondary star is comparable to that of the primary component. This motivates us to look for other possibilities.

### 3.2. An overcontact binary system

Given that to fit the observational data the secondary component in the case of semidetached system should have a luminosity nearly equal to that of the primary we propose an alternative model in which both stars are at the same evolutionary stage. However, we relax the assumptions of Santander-García et al. (2015) to allow for a more physically motivated solution. In particular, we assume that the position of Henize 2–428 in the Hertzsprung-Russell diagram corresponds to that of a model post-AGB star of mass  $\simeq 0.5 M_{\odot}$ , red line in Fig. 1. Thus, we adopt again  $T_{\text{eff},1} = 45,000$  K. We note that since this mass is very similar to that found when a semi-detached system is considered we keep the orbital separation at  $a = 1.27 R_{\odot}$ .

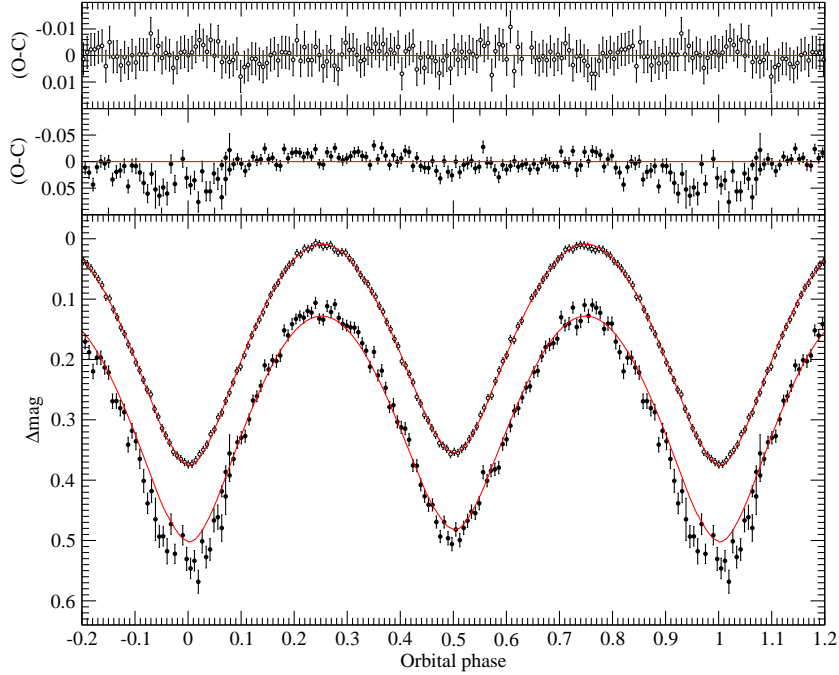


Figure 3: Light curve fits assuming an overcontact binary system made of two degenerate post-AGB cores. B- and I-band light curves are shown in the lower panel using filled and open circles, respectively. Red lines are the best-fit models for each band. Residuals are shown in the upper panels. Note the different scale for each band.

	Primary	Secondary
$M (M_{\odot})$	0.48 (0.22 – 1.50)	0.47 (0.22 – 1.48)
$R (R_{\odot})$	0.57 (0.44 – 0.84)	0.57 (0.44 – 0.83)
$r_{\text{pole}}$	0.400 (0.386 – 0.420)	0.397 (0.384 – 0.415)
$r_{\text{point}}$	contact	contact
$r_{\text{side}}$	0.431 (0.415 – 0.453)	0.426 (0.412 – 0.448)
$r_{\text{back}}$	0.495 (0.486 – 0.515)	0.490 (0.486 – 0.510)

Table 2: Absolute masses and volumetric radii derived from the best fit to light curves assuming an overcontact binary system. For each component, the radius relative to the semimajor axis is given in different directions accounting for deformation: towards the pole ( $r_{\text{pole}}$ ) and towards the companion direction ( $r_{\text{point}}$ ), opposite ( $r_{\text{back}}$ ), and perpendicular to the orbital plane ( $r_{\text{side}}$ ). Numbers in parentheses indicate the range of possible values corresponding to fits with  $0.8 \leq q \leq 1.2$  and  $1.0 \leq a \leq 1.9 R_{\odot}$ .

Additionally we did not take into account the mass ratio and the semi-major axis they derive because they are mainly constrained by the radial velocity fits, which we have argued that may not be related to the binary nature of the system. Nevertheless, the distance to the object and its luminosity may provide constraints on the scale of the binary system. Following our previous estimates in the case of a semi-detached binary, the total luminosity of the system is scaled by  $L = 845(D/1.4 \text{ kpc})^2 L_{\odot}$ . If we consider the independent distance measurements listed earlier in Sect. 2.2, Henize 2–428 may be at distance between 1.7 kpc and  $2.7 \pm 0.5$  kpc (Maciel, 1984; Frew et al., 2015). Then, the total luminosity of the system would be between 1,246 and 4,415  $L_{\odot}$ . We did not consider the distance estimate of (Santander-García et al., 2015), which is shorter, to keep our estimates independent of the light curve data we are using. Complementary, the total luminosity can also be computed from the effective temperatures, and relative radii derived from the light curve fits, along with the assumed semi-major axis. Therefore, the distance limits may provide constraints on the orbital semi-major axis.

Taking all this into account we have performed fits to the light curves assuming different values of mass ratio (from 0.5 to 1.5) and semi-major axis (from 1.0 to 2.0  $R_{\odot}$ ), fixing  $T_{\text{eff},1} = 45,000$  K. The resulting light curves for our best fit model are shown in Fig. 3, and the physical parameters of the binary system are listed in Table 2. We note that, as expected, neither the semi-major axis nor the mass ratio have a significant impact on the quality of the fits at the level of precision of the light curves. However, they have an obvious impact on the absolute properties of the system. On the one hand, the absolute radius of each component is proportional to  $a$ , which defines the scale of the system. On the other hand, the relative size of each component ( $r$ , derived from the pseudo-potential) is correlated with the mass ratio because the stars of the binary are in contact. From the relative radii, the effective temperature and the semi-major axis, we computed the total luminosity of the system for each fit ( $L \simeq (ar)^2 T_{\text{eff}}^4$ ). The results show that the previously computed luminosity limits are consistent with a semi-major axis ranging from 1.0 to 1.9  $R_{\odot}$ , almost independently of the value of the mass ratio. Given the period of the system, this can be translated into a total mass of the system in the range  $\simeq 0.45 - 3.0 M_{\odot}$ . If we assume a mean measured distance of 2.2 kpc, then  $a \simeq 1.3 R_{\odot}$  and the total mass would be  $\simeq 1.0 M_{\odot}$ , in agreement with the position of the system on the Hertzsprung-Russell diagram.



Given that the relative size of the components correlates with the mass ratio of the system, we have run fits by fixing  $a = 1.3 R_{\odot}$  and setting the mass ratio as a free parameter. The best fit is found for  $q = 0.98 \pm 0.20$ , very close to the ratio adopted by Santander-García et al. (2015), although it is poorly constrained by the light curves. As can be seen in Fig. 3, for this model the agreement between the theoretical light curves and the observed ones is excellent, both in the B-band and in the I-band, being the residuals very small, 16.93 mmag and 3.25 mmag, respectively. For the best fit model, the inclination of the system is  $i = 63.2^{\circ}$  and the effective temperature of the secondary star is  $T_{\text{eff},2} = 41,100$  K. These parameters yield the masses of both components of the binary system,  $0.48 M_{\odot}$ , and  $0.47 M_{\odot}$ . Thus, the total mass of the binary system is  $0.95 M_{\odot}$ , well below the Chandrasekhar limiting mass. Hence, even if the system is made of two post-AGB stars, the total combined mass of the system will not be enough to produce a Type Ia supernova outburst, as Santander-García et al. (2015) claimed. In any case, stars with these properties are most probably post-AGB stars, and the component of lower mass is likely to be a helium white dwarf.

Nevertheless, we stress here that the absolute properties of the components of Henize 2–428 are only roughly constrained by the light curve fits if we take into account the range of mass ratios and orbital semi-major axes that produce comparable fits to the light curves. Table 2 shows the properties of the best fit described above, with the range of possible values associated to the mass ratio and semimajor axis uncertainties. Although the combined analysis of light curves and the position in the Hertzsprung–Russell diagram favor a scenario of two similar stars with masses  $\simeq 0.5 M_{\odot}$ , only precise radial velocities can better constrain the model.

#### 4. Summary and conclusions

We addressed the recent claim made by Santander-García et al. (2015) that the central binary system of the planetary nebula Henize 2–428 is a SN Ia progenitor in the frame of the double-degenerate scenario. This claim has attracted some attention, and if true it would be the first super-Chandrasekhar mass binary white dwarf system with short period discovered ever. More interestingly, it would be definitely located in the center of a planetary nebula, providing strong evidence for SN Ia occurring inside PNe, termed SNIPs (Tsebrenko & Soker, 2015). However, we found that, although certainly possible, this claim is not yet univocally supported by the observations, and that

different explanations are possible, and need to be considered.

Our statement is based not only on purely theoretical considerations about the evolutionary properties of the central object of Henize 2–428, but also on the way the observed data set has been analyzed. In particular, in Sect. 2 we argued that the claim for an equal-masses binary system and the required mass, luminosity, and radius of the two stars does not comply with evolutionary tracks of post-AGB stars (see Fig. 1). We also analyzed critically the way in which observations were interpreted, and we questioned the two most important assumptions made to study the observed properties of the binary system at the center of Henize 2–428. These are that both components of the binary system have exactly the same mass, and that, moreover, they are at the same evolutionary stage.

In particular, in Sect. 2.2 we argued that there are strong theoretical arguments that pose a problem to the scenario proposed by Santander-García et al. (2015). One of these arguments is that the initial mass difference in the main sequence must be very small. The second one is that the population of twin binaries is small. Furthermore, in Sect. 2.3 we critically examined the joint analysis of the light curves and the spectrum of Santander-García et al. (2015). Specifically, we argued that the explanation of Santander-García et al. (2015) of the variability of the He II 5412 Å absorption spectral line as arising from Doppler shifts of two absorption lines, one from each star, is not the only possible one. Instead, we suggested that the variability of the He II 5412 Å spectral line can be accounted for by a, possibly time-varying, broad absorption line from the central star on top of which there is a time-varying narrow emission line from the compact nebula or even from much closer to the star. Dobrincic et al. (2008) find the age of the Henize 2-428 equatorial ring to be  $4,300(D/1.8 \text{ kpc}) \text{ yr}$ . Although the ring is old, there is a compact dense nebula near the central star (Rodríguez et al., 2001). It is quite possible that the He II 5412 Å narrow emission spectral line sitting on top of the broad absorption line originates in the compact nebula, or from an outflow that feeds the compact nebula much closer to the star. This explanation could also be compatible with the observed spectrum, but more detailed studies and better observations are needed to resolve in detail the spectral feature.

All these considerations led us to judge that although the first of the assumptions of Santander-García et al. (2015) – namely, that both stars have approximately the same mass – is quite possible, the second one – that both components of the binary system are at exactly the same evolutionary stage

– is not fully justified, and needs an independent evaluation. Since these two assumptions are quite restrictive, we explored alternative models. Accordingly, we analyzed other possible explanations, less extraordinary but that could fit equally well the observations and, simultaneously, do not contradict stellar evolutionary results (Sect. 3).

The first of these scenarios still hold the existence of a binary system, as the two (almost) symmetric broad minima in the light curve are attributed to tidal distortion caused by a companion of similar mass. In particular, we mentioned a binary system composed of either a post-RGB or a post-AGB star with a low-mass companion. In the first case, a low-mass main sequence star truncates the evolution of a star of initial mass  $M_{\text{ZAMS}_1} \approx 1.0 M_{\odot}$  on the upper RGB. In the second scenario, a main sequence star truncates the evolution of a star of initial mass  $M_{\text{ZAMS}_1} \approx 2.5 - 3.0 M_{\odot}$  on the lower AGB. However, we found that although this model is plausible it does not fit well the observed light curves. Consequently, we studied a second possibility in which the assumptions of Santander-García et al. (2015) are relaxed. We found that a binary system made of two post-AGB stars of masses  $0.453 M_{\odot}$  and  $0.437 M_{\odot}$  can fit equally well the observed light curve of the system. Hence, if our interpretation of the observed data is correct the combined mass of the binary system would be below Chandrasekhar’s limiting mass, and it would not explode as a SN Ia. We conclude this short study by stating that the exact nature of the central object of Henize 2–428 is still to be determined.

## Acknowledgements

We acknowledge useful discussions with Miguel Santander-García, who also supplied us unpublished data. This research was partially supported by MINECO grant AYA2014-59084-P, by the AGAUR (EG-B), by the AGENCIA through the Programa de Modernización Tecnológica BID 1728/OCAR, and by the PIP 112-200801-00940 grant from CONICET (LGA). IR acknowledges support from the MINECO and the Fondo Europeo de Desarrollo Regional (FEDER) through grants ESP2013-48391-C4-1-R and ESP2014-57495-C2-2-R.

## References

Althaus, L. G., Miller Bertolami, M. M., & Córscico, A. H. 2013, *A&A*, 557, AA19

- Aznar-Siguán, G., García-Berro, E., Lorén-Aguilar, P., José, J., & Isern, J. 2013, *MNRAS* , 434, 2539
- Bloecker, T. 1993, *Acta Astro.*, 43, 305
- Bloecker, T., & Schoenberner, D. 1991, *A&A* , 244, L43
- Cahn, J. H., & Kaler, J. B. 1971, *ApJS* , 22, 319
- Cantrell, A. G., & Dougan, T. J. 2014, *MNRAS* , 445, 2028
- Chiosi, E., Chiosi, C., Trevisan, P., Piovan, L., & Orío, M. 2015, *MNRAS* , 448, 2100
- Claret, A. 2000a, *A&A* , 363, 1081
- Claret, A. 2000b, *A&A* , 359, 289
- Dickel, J. R., & Jones, E. M. 1985, *ApJ* , 288, 707
- Dobrincic, M., Villaver, E., Guerrero, M. A., & Manchado, A. 2008, *AJ* , 135, 2199
- Eggleton, P. P. 1983, *ApJ* , 268, 368
- Frew, D. J., Parker, Q. A., & Bojicic, I. S. 2015, arXiv:1504.01534
- García-Díaz, M. T., González-Buitrago, D., López, J. A., Zharikov, S., Tovmassian, G., Borisov, N., & Valyavin, G. 2014, *AJ* , 148, 57
- Guerrero, M. A., Villaver, E., Manchado, A., Garcia-Lario, P., & Prada, F. 2000, *ApJS* , 127, 125
- Han, Z., & Podsiadlowski, P. 2004, *MNRAS* , 350, 1301
- Iben, I., Jr., & Tutukov, A. V. 1984, *ApJS* , 54, 335
- Iben, I., Jr., & Tutukov, A. V. 1985, *ApJS* , 58, 661
- Kashi, A., & Soker, N. 2011, *MNRAS* , 417, 1466
- Kushnir, D., Katz, B., Dong, S., Livne, E., & Fernández, R. 2013, *ApJ* , 778, L37

- Livio, M., & Riess, A. G. 2003, *ApJ* , 594, L93
- Livne, E., & Arnett, D. 1995, *ApJ* , 452, 62
- Lucy, L. B., & Ricco, E. 1979, *AJ* , 84, 401
- Lucy, L. B. 2006, *A&A* , 457, 629
- Maciel, W. J. 1984, *A&A Supp. Series*, 55, 253
- Maoz, D., Mannucci, F., & Nelemans, G. 2014, *ARA&A* , 52, 107
- Nomoto, K. 1982, *ApJ* , 253, 798
- Paczyński, B. 1970, *Acta Astronomica*, 20, 47
- Pinsonneault, M. H., & Stanek, K. Z. 2006, *ApJ* , 639, L67
- Prinja, R. K., & Urbaneja, M. A. 2014, *MNRAS* , 440, 2684
- Raskin, C., Timmes, F. X., Scannapieco, E., Diehl, S., & Fryer, C. 2009, *MNRAS* , 399, L156
- Renedo, I., Althaus, L. G., Miller Bertolami, M. M., et al. 2010, *ApJ* , 717, 183
- Rodríguez, M., Corradi, R. L. M., & Mampaso, A. 2001, *A&A* , 377, 1042
- Santander-García, M., Rodríguez-Gil, P., Corradi, R. L. M., Jones, D., Miszalski, B., Boffin, H. M. J., Rubio-Diez M. M., & Kotze, M. M. 2015, *Nature*, 519, 63
- Santander-García, M., Rodríguez-Gil, P., Jones, D., Corradi, R. L. M., Miszalski, B., Pyrzas, S., & Rubio-Diez, M. M. 2011, *Asymmetric Planetary Nebulae 5 Conference*, 259
- Shen, K. J., Guillochon, J., & Foley, R. J. 2013, *ApJ* , 770, L35
- Soker, N. 1996, *ApJ* , 460, L53
- Soker, N., Kashi, A., García-Berro E., Torres, S., & Camacho, J. 2013, *MNRAS* , 431, 1541
- Thompson, T. A. 2011, *ApJ* , 741, 82

- Todt, H., Kniazev, A. Y., Gvaramadze, V. V., et al. 2013, MNRAS , 430, 2302
- Tsebrenko, D., & Soker, N. 2013, MNRAS , 435, 320
- Tsebrenko, D., & Soker, N. 2015, MNRAS , 447, 2568
- Wang, B., & Han, Z. 2012, NewAR, 56, 122
- Webbink, R. F. 1984, ApJ , 277, 355
- Weidmann, W. A., & Gamen, R. 2011, A&A , 531, AA172
- Whelan, J., & Iben, I., Jr. 1973, ApJ , 186, 1007
- Wilson, R. E. 1979, ApJ , 234, 1054
- Wilson, R. E., & Devinney, E. J. 1971, ApJ , 166, 605
- Woosley, S. E., & Weaver, T. A. 1994, ApJ , 423, 371